fluids

MDPI

Article

Experimental Particle Image Velocimetry Apparatus with Known Displacement of Synthetic Particles

Anderson Gomes Girardi *, Sigeo Kitatani Júnior, João Paulo da Silva Fonseca * and Felipe Pamplona Mariano

Laboratório de Mecânica Aplicada (LABMEC), Escola de Engenharia Elétrica, Mecânica e de Computação (EMC), Universidade Federal de Goiás (UFG), Goiânia 74690-900, GO, Brazil; sigeojr@ufg.br (S.K.J.); fpmariano@ufg.br (F.P.M.)

* Correspondence: andersongomes@ufg.br (A.G.G.); jpsfonseca@ufg.br (J.P.d.S.F.)

Abstract: The study of velocimetry is important for characterizing and comprehending the effects of fluid flow, and the particle image velocimetry (PIV) technique is one of the primary approaches for understanding the velocity vector field in a test section. Commercial PIV systems are expensive, with one of the main cost factors being high-speed camera equipment capable of capturing images at high frames per second (fps), rendering them impractical for many applications. This study proposes an evaluation of utilizing smartphones as accessible image acquisition systems for PIV technique application. An experimental setup inspired by the known angular displacement of synthetic particles is proposed. A stepper motor rotates a plate containing an image of synthetic particles on its surface. The motion of the plate is captured by the smartphone camera, and the images are processed using PIVlab-MatLab® software. The use of two smartphones is assessed, with acquisition rates of either 240 fps or 960 fps and varying angular velocities. The results were satisfactory for velocities up to 0.7 m/s at an acquisition rate of 240 fps and up to 1.8 m/s at 960 fps, validating the use of smartphones as a cost-effective alternative for applying the PIV technique, both for educational purposes and for research carried out in low-income organizations.

Keywords: PIV; image acquisition; measurement; smartphone; high-speed camera; low-cost

check for updates

Academic Editors: Jun Yao, Mingming Ge, Guangjian Zhang and Xin-Lei Zhang

Received: 30 October 2024
Revised: 10 March 2025
Accepted: 12 March 2025
Published: 16 March 2025

Citation: Girardi, A.G.; Júnior, S.K.; Fonseca, J.P.d.S.; Mariano, F.P. Experimental Particle Image Velocimetry Apparatus with Known Displacement of Synthetic Particles. *Fluids* **2025**, *10*, 68. https://doi.org/10.3390/fluids10030068

Copyright: © 2025 by the authors. Licensee MDPI, Basel, Switzerland. This article is an open access article distributed under the terms and conditions of the Creative Commons Attribution (CC BY) license (https://creativecommons.org/licenses/by/4.0/).

1. Introduction

Velocimetry is extremely important for characterizing and understanding the effects of fluid flow. Several techniques are applied in studying velocimetry, with it being possible to mention punctual and global applications capable of measuring the velocity of a point, or of the entire flow field.

Some of the most popular contemporary techniques include the Pitot tube, rotating vane anemometry, hot wire or hot film anemometry, hot sphere anemometry, ultrasonic anemometry and laser Doppler velocimetry. The global techniques mainly include particle image velocimetry (PIV), particle tracking velocimetry (PTV) and particle shadow velocimetry (PSV), all based on optical principles. Detailed descriptions of the mentioned techniques can be seen in the literature [1–3].

Particle image velocimetry (PIV) is a widely used technique for mapping velocity fields in fluids. Its applications range from academic studies to industrial applications. However, the high cost of commercial PIV systems, including high-speed cameras and pulsed lasers, represents a significant barrier for institutions with limited resources. Recent studies [4–7] have investigated affordable alternatives, such as action cameras and smartphones, which have the potential to democratize the use of this technique, particularly in educational

contexts. The study [6] showed promising results when employing low-cost devices in PIV experiments, highlighting its feasibility for use in flow with velocities up to 1 m/s, while the work [7] evaluated flows with velocities up to 3.5 m/s.

Specifically considering the PIV technique, it is defined as a measurement technique that allows for capturing velocity fields in fractions of a second [8]. The velocity distribution in a whole field of a fluid flow is determined by measuring the displacements that the images of tracer particles experience during a time interval. Naturally, the PIV is applied only for internal flow measurements, including wind tunnel flows, gas flow in an internal combustion engine cylinder, laminar flames, waves, and turbulent channel flows [9]. A previous study [10] mentioned that PIV complete commercial systems are produced by just a few suppliers in the world trade. In addition, acquiring a commercial PIV measurement system represents a high cost for many institutions, and thus makes the acquisition unfeasible even for large companies or research and teaching centers.

As regards the advantages of applying the PIV technique, the literature [7–9] indicates developments in the direction of building experimental configurations with alternative resources and more accessible cost. These systems can be used for educational applications, or even to meet the requirements of certain research.

For example, these systems include using a smartphone camera with 240 frames per second (fps) to capture images in flowing water [4], applying an action camera (GoPro Hero 5) to analyze the jet flow of an aquarium pump filled with water [10], and working with four smartphones to capture images and perform velocimetry processing of TOMO-PIV tomographic particle images [9].

A camera with a high image acquisition rate is essential in the process among the devices necessary to constitute the PIV technique, mainly for air flows in a wind tunnel, since the flow velocity is normally higher when compared to natural hydraulic flow velocities.

To develop a low-cost PIV measurement technique applied in a wind tunnel, it is desirable to use a system for image acquisition that is accessible and versatile, and which can capture images with a suitable acquisition rate. In this direction, the literature indicates the development of experimental apparatus based on synthetic particle displacement to simulate the flow of particles with known displacement and to evaluate the use of alternative equipment for image acquisition. For example, a study [5] reports the use of a plate with a 100 mm diameter in controlled rotation from 1.5 to 4 Hz, capturing images with a GoPro Hero 5 action camera. Another study [7] reported the use of a plate with synthetic particles for experimental validation during the development of the SmartPIV software, version 1.2.1 (https://smartpiv.app/), available for smartphones with Android and IOS systems.

Thereby, this study proposes to test the viability to use smartphones as image acquisition systems for the PIV technique. So, an experimental apparatus inspired by the angular displacement of particles was built, in this case by the synthetic printing of particles on the face of a plate coupled to a motor shaft. The images were acquired using two smartphones from different manufacturers, and subsequently processed by MatLab® software, version R2022a 9.12 (https://www.mathworks.com/), using the PIVlab tool, version 2.61 (https://www.pivlab.de/). Through the suggested method, it is possible to establish a particle displacement pattern according to an adjustment of the angular velocity of the plate with printed particles. Thus, with the known displacement pattern, it is possible to evaluate only specific characteristics of the experimental apparatus.

Although the PIV technique is widely used, its high cost and complexity limit its application in low-resource institutions. Alternatives such as the use of action cameras and smartphones have been explored to democratize this technique, but there are still gaps in the critical evaluation of its accuracy and applicability. This study seeks to fill this gap by

experimentally validating an apparatus based on the angular displacement of synthetic particles, analyzing the influence of the image acquisition rate on the accuracy of the results. Thus, this work is positioned within the broader context of PIV research, highlighting the advantages and limitations of the proposed method and contributing to the definition of guidelines for the effective use of accessible devices.

Future studies can explore the feasibility of extending this low-cost approach to low-velocity flow-based PIV, opening up new possibilities for the measurement of multiphase flows in which densitometry is essential. Ref. [11] used the PIV technique to measure the velocity field in an oil–water two-phase flow with high water fraction and low velocity in a small-diameter horizontal pipe. Furthermore, it is possible to verify the feasibility of using the combination of the PIV technique using a smartphone together with the synchrotron X-ray microimaging method used to observe internal structures. Ref. [12] used the synchrotron X-ray PIV technique combined with an optical array and a CCD camera to investigate the characteristics of blood flow in a circular pipe.

Finally, this work proposes an innovative approach to validate the use of smartphones as image acquisition systems for the PIV technique. In addition to exploring the speed and resolution limits, we seek to highlight the simplicity and accessibility of the method for educational and academic purposes, contributing to the teaching of fundamental concepts of fluid dynamics.

2. Materials and Methods

An experimental setup was developed to investigate fluid dynamics using PIV. The system incorporated affordable and accessible equipment, including stepper motors and smartphones, to capture the motion of synthetic tracer particles. This setup aimed to evaluate the feasibility of using simple, low-cost technology for high-precision fluid flow measurements. The method employed optimized image acquisition and processing techniques to ensure accuracy and repeatability, offering a practical alternative to more complex and expensive systems commonly used in fluid dynamics studies.

Although this study focuses on validating the use of smartphones for PIV measurements under controlled conditions, its applicability can be extended to more complex scenarios, even being used to study low-velocity flows, for a variety of applications, including the investigation of the flow around wind turbines [13], the analysis of aerodynamic profiles [14], and the visualization of flow patterns in channels [15]. Likewise, its use extends to thermal studies, such as natural convection in closed environments [16], and the analysis of flows over porous or rough surfaces [17].

2.1. Experimental Setup

The proposed experimental apparatus uses a National Electrical Manufacturers Association (Rosslyn, VA, USA) (NEMA 17) standard stepper motor, type KH42JM2B14OE from Japan Servo Co. (Tokyo, Japan), with a resolution of 200 steps per revolution and a step angle corresponding to 1.8 angular degrees. A rigid flange made of Nylon was coupled to its motor shaft and an MDF plate were mounted at the end. The Nylon flange consists of a threaded coupling element, which facilitates interchanging plates, since each plate may have attached to it an image representing particles of different sizes and geometric spreading.

The power supply and control system consist of a 24VDC voltage source, model EQE12010005, a programmable logic controller (PLC), model DVP-14SS2, both from Delta Eletronics (Neihu District, Taipei, Taiwan) and a stepper motor drive, model MD508D from Metaltex (Vila Mangalot, São Paulo, SP, Brazil). A digital tachometer, model TD-813 from Instrutherm (Vila Santa Delfina, São Paulo, SP, Brazil), was installed at the bottom of the

plate so that it would be possible to measure the angular velocity in revolutions per minute (RPM) with the use of a reflective tape attached to the bottom of the plate. A smartphone is positioned on an MDF support above the plate, and the focal length for capturing images can be easily changed by vertically adjusting the support base.

The experiments were carried out using a set of professional continuous lighting for photographs and filming in order to standardize the lighting in the environment, consisting of a soft box with dimensions of 0.5 m × 0.7 m and a spiral fluorescent lamp with 135 W of power and temperature of 5500 K color, known as daylight, which is quite widely used for photo studios. Details of the configured experimental apparatus and its components can be seen in Figure 1.

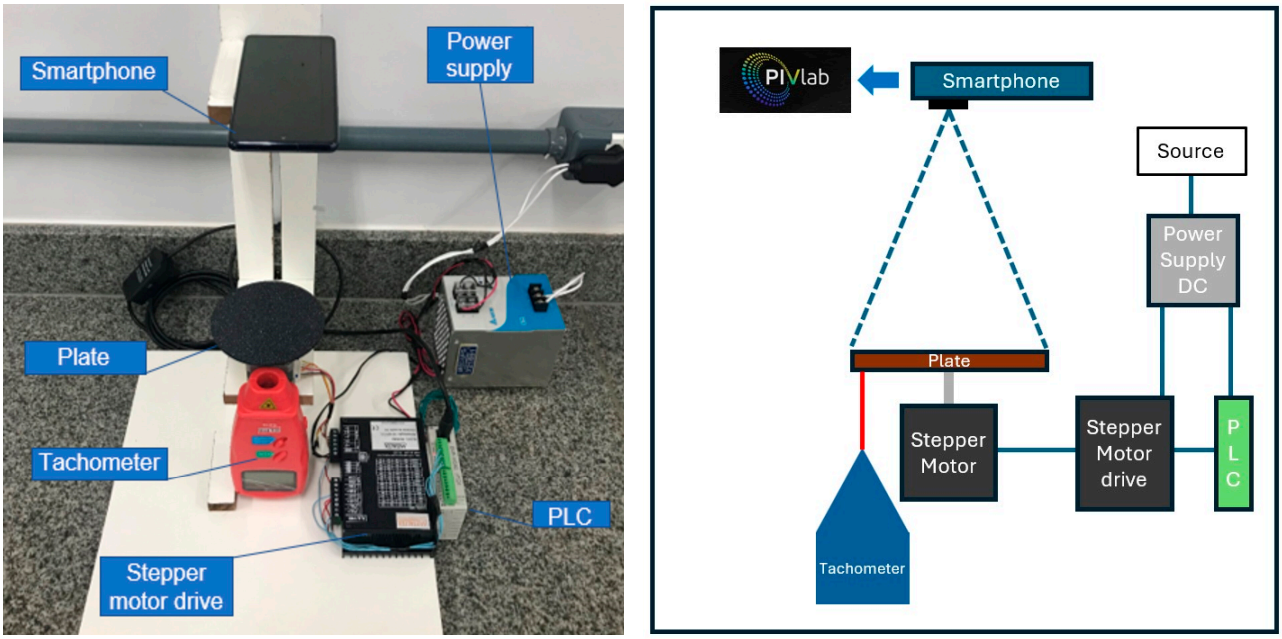

(**a**) (**b**)

Figure 1. (**a**) Image of the Experimental setup and its components; (**b**) Schematic representation of the experimental setup.

2.2. Tracer Particles

According to the guidelines on the best practices for applying PIV [18], the particles must be able to form visible images under certain lighting conditions; in addition, they must have the ability to accurately follow the fluid movement without influencing the flow and be able to mark enough points in space to effectively resolve spatial flow.

Thus, the correct addition of tracer particles in the fluid is essential for achieving greater accuracy in vector field velocimetry results. The use of synthetic particles consists of a practical method of evaluating the image acquisition system in applying the PIV technique without the need to worry about the generation and feeding of tracer particles.

The images with synthetic particles were generated using the PIVlab-MatLab® application, through which it is possible to configure different parameters to change the particle concentration and size, as shown in Figure 2.

A particle diameter optimization study [8] observed that particles with a diameter of approximately 2 pixels presented results with lower measurement uncertainty in the digital evaluation of PIV. Another study [19] evaluated the influence of synthetic particle diameter, obtaining the smallest mean errors for particles with diameters between 1.0 and 3.0 pixels. Recently [4], images of synthetic particles with 2.5 pixels of diameter were used to evaluate the PIV technique using a smartphone.

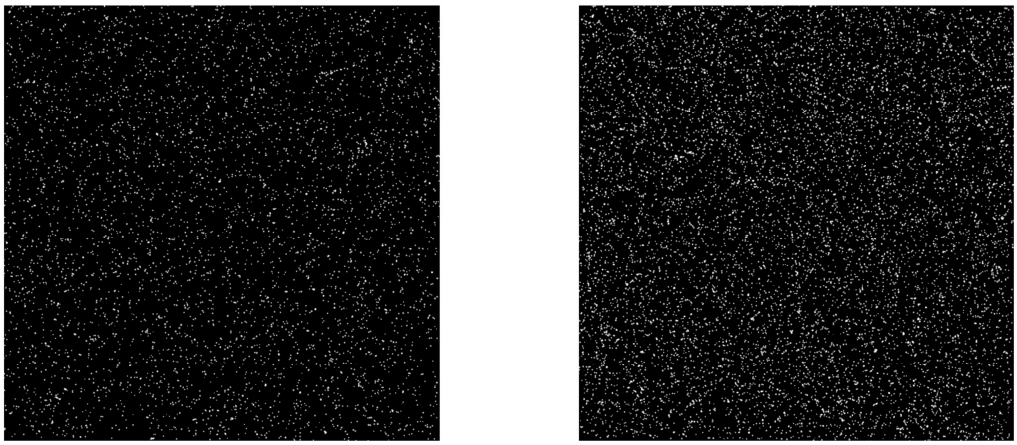

Resolution: 720 × 720 px
Number of particles: 5000
Particle diameter: 2 px
(**a**)

Resolution: 720 × 720 px
Number of particles: 10,000
Particle diameter: 3 px
(**b**)

Figure 2. Example of image composed of different particle concentrations and sizes, made using the PIVlab-MatLab® synthetic particle image generator: (**a**) lower particle density and (**b**) higher particle density.

In addition to the parameter associated with particle size, particle concentration is quite relevant for the PIV technique, and a concentration of about 10 particles per interrogation area was recommended [20]. Based on data from the literature, the PIVlab-MatLab® synthetic particle image generator was used to compose the images shown in Figure 2, which were reproduced on a laser printer with a sheet of 75 g alkaline bond paper and subsequently attached on an MDF plate 3 mm thick and 100 mm in diameter, as shown in Figure 3.

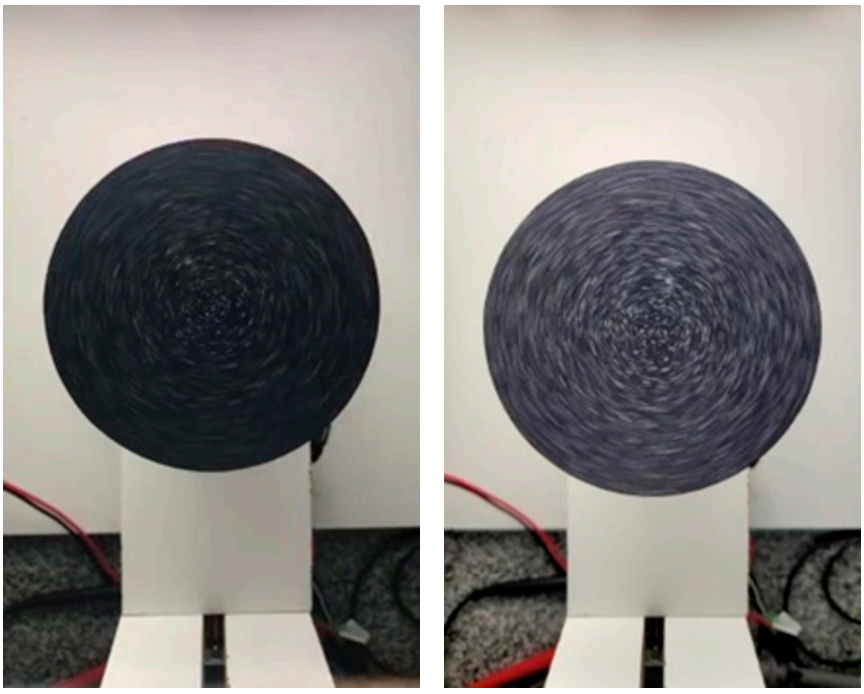

(**a**) (**b**)

Figure 3. (**a**) Frame acquired using the image acquisition systems IS1; (**b**) Frame acquired using the image acquisition systems IS2.

2.3. Image Acquisition System

Image acquisition was performed using portable equipment that is easily accessible on the market. With technological advances, smartphones equipped with cameras capable of recording images at up to 960 fps are easily available, thereby enabling us to evaluate their use as a tool in acquiring images for the PIV technique. Inspired by this technological capacity and similar works found in the literature [4–6], it was proposed to evaluate the applicability of two devices as image acquisition systems for the PIV technique.

The first tests used an Apple iPhone 7 smartphone (Apple Campus, Cupertino, CA, USA), named in this study as image sensor 1 (IS1), capable of recording videos in slow motion with 240 fps and a resolution of 720 × 1280 pixels. A Samsung S20 Fe smartphone (SAMSUNG, Suwon-si, Republic of Korea) was subsequently used, named in this study as image sensor 2 (IS2), with a slow-motion recording capacity of 240 fps and resolution of 1080 × 1920 pixels, in addition to the Super Slow-Motion (SSM) mode with the ability to record at 960 fps and resolution of 720 × 1280 pixels.

The videos were recorded in .MP4 format and loaded into the PIVlab-MatLab® application, which identifies the number of frames and the resolution of the video. It is also possible to visualize the frames and select the start and end range of the frames to be loaded for processing in this application using the PIV technique. It is noteworthy that the recording mode time for the IS2, when using the SSM mode, is limited to 0.5 s, and despite the short recording period, this is not a limiting factor for image processing using the PIV technique, since it obtains a video with approximately 560 frames. Several studies [21–25] used up to 500 frames to process the PIV technique. Furthermore, the sensitivity of the digital sensor of the IS1 and IS2 cameras was not changed, since this configuration is not accessible to the smartphone user in the SM and SSM functions, thus maintaining the manufacturer's default configuration.

According to the experimental configuration (Figure 1), the IS1 was positioned 190 mm above the target and the field of view (FOV) obtained was 115 mm × 205 mm. Next, the complete framing of the plate with a diameter of 100 mm was performed in this configuration. An FOV was established with a minimum edge of 5% free of the moving object around the entire perimeter of the plate, as preliminary tests pointed out flaws in the result when the vector field under analysis was close to or coincident with the FOV limit. Thus, it is possible to see in Figure 3 that the captured field of view covers the entire plate image and a free area around its perimeter. Under these conditions, the spatial resolution obtained was 39.09 pixels/mm^2, which corresponds to a linear pixel length of 160 µm.

When using IS2 for slow-motion recording at 240 fps, the FOV obtained was 135 mm × 240 mm, while the spatial resolution was 64 pixels/mm^2, which corresponds to a linear pixel length of 125 µm. When using IS2 in SSM mode recording at 960 fps and maintaining the target positioning distance of 190 mm, the FOV was maintained at 135 mm × 240 mm, but the spatial resolution reached 28.44 pixels/mm^2, corresponding to the linear pixel length of 187 µm. It is possible to observe a comparison between the main characteristics of the image acquisition systems IS1 and IS2 in Table 1.

According to the guidelines on best practices for applying PIV/SPIV in towing tanks and cavitation tunnels [11], the nominal spatial resolution value is between 5 and 20 pixels/mm^2, and consequently the pixel length is between 223 µm to 447 µm. However, another studies [24–28] considered applying the PIV technique in a wind tunnel with a different FOV, and here the pixel length varies between 5 µm and 200 µm.

Therefore, it can be said that the use of IS2 and IS1 as image acquisition systems applied in the proposed experimental setup (Figure 1) guarantees processing conditions beyond those provided for applying PIV/SPIV in towing tanks and cavitation tunnels [18], considering that image processing and analysis becomes more accurate the smaller the

pixel length. In addition, the pixel length acquired in the settings falls within the range of sizes reported in the literature [24–28] for applying the PIV technique in a wind tunnel.

Table 1. Experimental parameters obtained in the setup of the IS1 and IS2 image acquisition systems.

Smartphone	**iPhone 7—IS1**	**Samsung S20 Fe—IS2**	
Acquisition mode	Slow-motion camera	Slow-motion camera	Super slow-motion camera
Frame rate (fps)	240	240	960
Resolution (pixel)	720 × 1280	1080 × 1920	720 × 1280
Field of view (FOV) (mm)	115 × 205	135 × 240	135 × 240
Spatial resolution (pixel/mm^2)	39.08	64	28.44
Pixel length (µm)	159	125	187

2.4. Processing System

The PIVlab-MatLab® (version 2.56) application [29] was used to perform the processing. Images acquired with both acquisition systems (IS1 and IS2) were analyzed with the same settings.

The IS2's SSM function includes video acquisition limited to approximately 560 frames. The frameset was strategically divided into 3 parts of 180 frames, so the first and last thirds of the frameset were discarded, using only the central interval for processing. As the videos obtained in the IS1 and in the slow-motion mode of the IS2 do not have a recording time limitation, and consequently a limited number of frames, an acquisition time of approximately 5 s was defined using the central interval of 180 frames for analysis.

As the objective of this study is to evaluate the movement of the synthetic particles describing a known trajectory, an exclusion mask of the field external to the image of the plate in movement was created. Therefore, the processing result will only be presented in the area of interest of the plate's rotational movement. In addition, it is possible to save computational processing time.

Time-resolved particle image velocimetry (TR-PIV) is based on a comparison between two subsequent images. It is possible to obtain the vector field of a given region through displacement and time variation between images. Several types of algorithms can estimate the displacement of a group of particles using cross-correlation techniques. The PIVlab-MatLab® application has three options of algorithms that can be used to perform the processing; in this study, the selected algorithm applies the cross-correlation function through the Fast Fourier Transform (FFT) method.

To configure this algorithm, it is necessary to scale the interrogation subareas with square dimensions (for example, 64 × 64, 32 × 32, 16 × 16 pixels) and also apply an overlapping factor. In addition, it is possible to perform multi-pass processing, which increases the probability of achieving greater accuracy in the results [29].

On the other hand, the PIVlab-MatLab® software has the option "configuration suggestion" to define the interrogation area. A quadrant within the FOV is selected and the algorithm measures particle size and concentration to propose a recommended interrogation area. The configuration is implemented through averaging based on displacement, particle quantity and experimental practice. In the configuration of the processing system of this study, the multi-pass method was used, with dimensions of 64 × 64, 32 × 32, 16 × 16 pixels.

The methods were carefully structured to ensure replicability and comprehensibility, and the parameters were optimized based on recommendations in the literature and preliminary tests. Although the goal is not to compete with high-precision commercial systems, the presented methodology seeks to balance simplicity, affordability, and functionality.

3. Results

This study is divided into three different analyses. Section 3.1 analyzes the ability to use two different smartphones for image acquisition via the PIV technique. Section 3.2 verifies the capacity of a single smartphone depending on changing the camera capture speed. Finally, in Section 3.3, we evaluate the acquisition capacity of the smartphone with the highest acquisition rate due to the increase in the velocity of synthetic particles.

3.1. Comparative Analysis for Different Image Acquisition System

To analyze the velocimetry of particles with known displacement using the processing concepts of the PIV technique and the possibility of using easily accessible cameras, images were acquired with two different smartphone models: an Apple iPhone 7, called IS1, and a Samsung Galaxy S20 Fe, called IS2, both configured to capture images at a rate of 240 fps.

The synthetic image shown in Figure 2b was considered to simulate the flow of particles. The angular speed of the plate was adjusted to 90, 180 and 360 RPM, whose values were previously calibrated using the tachometer, with accuracies of $\pm(0.05\% + 0.1$ RPM). The application configuration used to perform the processing followed the Fast Fourier Transform (FFT) method, and the interrogation window was selected with three multi-passes (64×64, 32×32, and 16×16 pixels) with 50% overlap.

The qualitative results are shown in Figure 4. The tangential velocity vectors for 90 RPM (Figure 4a,d) and 180 RPM (Figure 4b,e) are zero near the center, and increase in magnitude when moving to the edge of the plate.

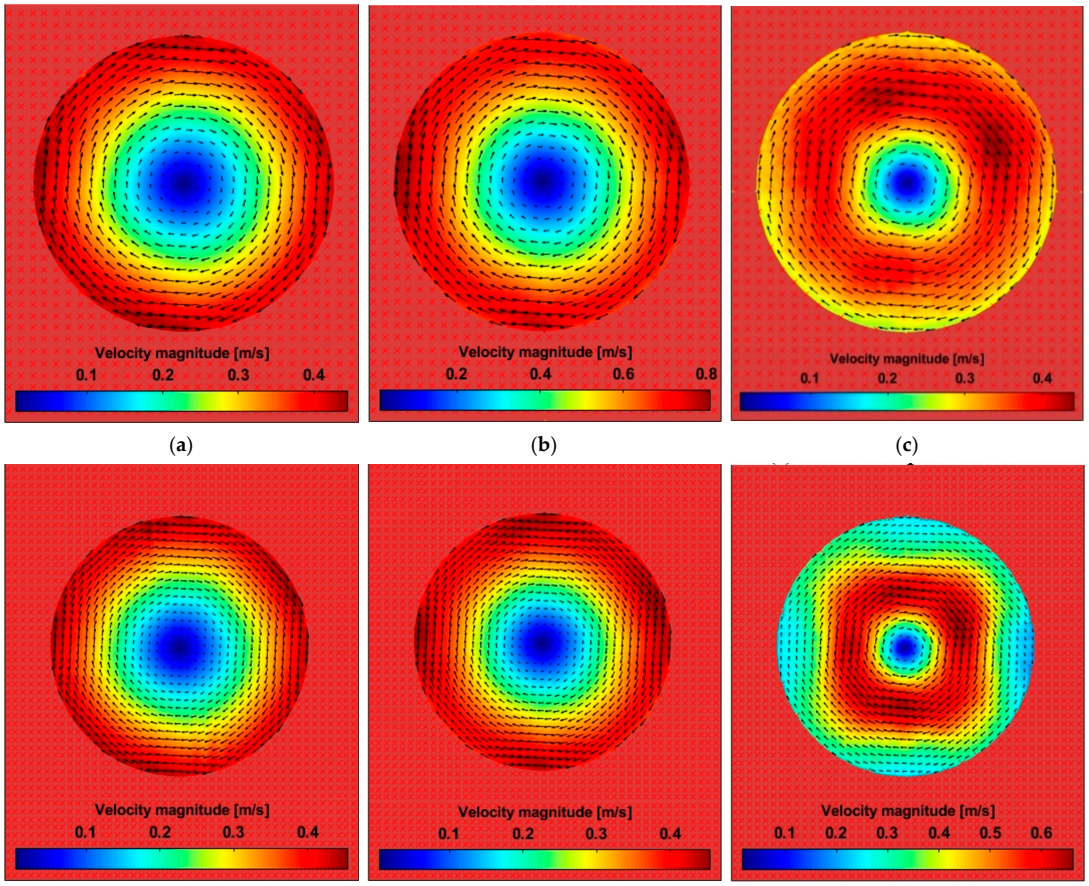

Figure 4. Velocity field obtained with the PIVlab-MatLab® application from images captured by the two acquisition systems for three different angular velocity settings and an acquisition frequency of 240 fps: (**a**) 90 RPM using IS1; (**b**) 180 RPM using IS1; (**c**) 360 RPM using IS1; (**d**) 90 RPM using IS2; (**e**) 180 RPM using IS2 and (**f**) 360 RPM using IS2.

On the other hand, at 360 RPM (Figure 4c,f), the velocity vectors reach the highest velocities in a region anterior to the edge of the plate. Moreover, a more pronounced drop in the magnitude of the tangential velocity vectors is observed for IS2 (Figure 4f) compared to IS1 (Figure 4c).

A quantitative analysis was performed by extracting vector data on an imaginary line, starting from the upper end of the circumference, passing through the center, and reaching the circumference's lower end. The theoretical tangential velocity of a rotating plate can be easily calculated from the rotation frequency and the size of the plate using Equation (1).

$$V_t = 2 \times \pi \times r \times f \quad (1)$$

where r is the radius of the plate in meters and f is the plate rotation frequency in rotation per second (RPS).

Thus, a curve was also generated with the estimated tangential velocity for the points coinciding with the axis of the straight line drawn using the MatLab® software program.

One of the current alternatives for verifying and validating the PIV technique involves using computational fluid dynamics (CFD). In this case, it is possible to determine an absolute uncertainty limit for each velocity vector, and a deviation of about ±10% between PIV and CFD techniques was considered in the studies reported in the literature [30,31].

The results of absolute tangential velocity derived using the PIV technique with the IS1 and IS2 acquisition systems, and the estimated tangential velocity for the angular velocities of 90 RPM, 180 RPM and 360 RPM, can be seen in Figure 5. In addition, the measurement deviation of ±10% in the estimated tangential velocity is represented with the dashed lines.

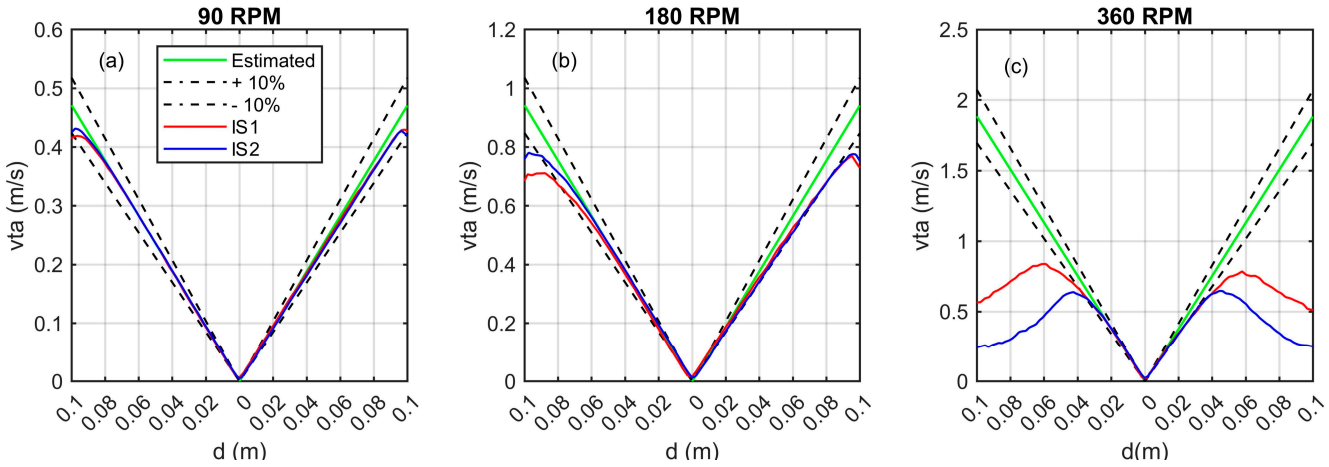

Figure 5. Analysis of velocimetry data for the configurations formed by IS1 and IS2 at 240 fps and plate angular velocities at (**a**) 90 RPM; (**b**) 180 RPM and (**c**) 360 RPM.

Figure 5a shows a good tangential velocity ratio for the entire evaluated section (the imaginary line) with an angular velocity of 90 RPM.

It can be seen in Figure 5b that the tangential velocity for 180 RPM showed a small deviation over the estimated value of about 0.8 m/s, close to the edge of the plate. A small difference can be identified at the upper edge of the plate between the results obtained with IS1 and IS2, with the values obtained by IS2 being closer to the estimated velocity.

The results for the angular velocity of 360 RPM are shown in Figure 5c. In this case, both the acquisitions, performed by IS1 and IS2, showed divergent results after 0.7 m/s, equivalent to position 0.04 m on the plate diameter. In other words, both smartphones were unable to acquire coherent images beyond 0.7 m/s.

After these analyses, the capacity for reliable representation of the tangential velocity vectors through processing with the PIV technique using smartphones is reduced with the increase in the angular velocity of the plate and according to the established experimental configurations. In addition, the two IS1 and IS2 models did not show significant differences that would influence the measurement range.

3.2. Comparative Analysis for Different Image Acquisition Speed

After comparing different image acquisition systems at a fixed acquisition rate (240 fps), this section presents the results obtained using only the IS2 smartphone, which offers different capture modes—slow motion (240 fps) and SSM (960 fps).

Thus, four tests were proposed with two angular velocity adjustments (180 and 360 RPM) for each available capture mode to evaluate the impact of increasing the acquisition rate. The following designations of (a)–(d) were applied for each test: (a) IS2—180 RPM—240 fps; (b) IS2—180 RPM—960 fps; (c) IS2—360 RPM—240 fps; (d) IS2—360 RPM—960 fps.

Figure 6 presents the results regarding the velocity fields obtained for the four proposed configurations.

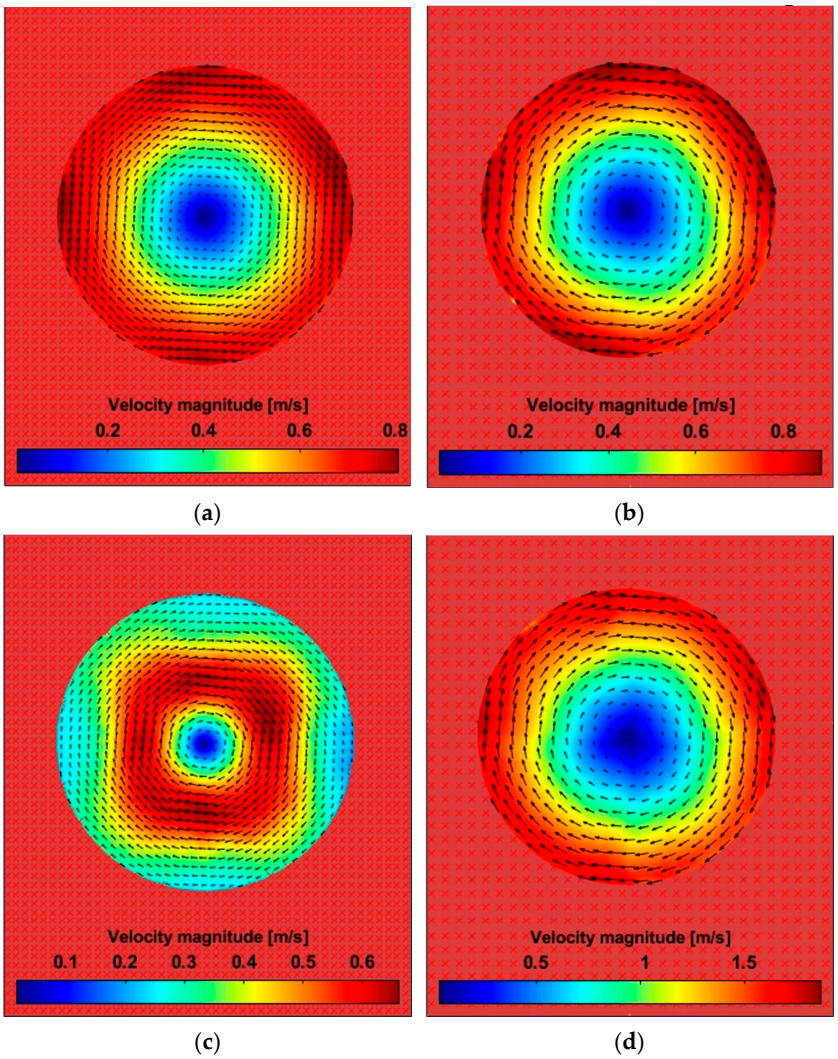

Figure 6. Velocity fields obtained with the PIVlab-MatLab® application from images captured with IS2 for different angular velocity (180 and 360 RPM) and acquisition frequency (240 and 960 fps) configurations: (**a**) 180 RPM and IS2 at 240 fps; (**b**) 180 RPM and IS2 at 960 fps; (**c**) 360 RPM and IS2 at 240 fps and (**d**) 360 RPM and IS2 at 960 fps.

Except for configuration (c), a positive gradient of vector fields from the center to the edges of the plate are observed. This evidences a limiting factor for applying the PIV technique considering an acquisition rate of 240 fps.

Figure 7 presents the graphical results of tangential velocity obtained with the PIVlab-MatLab® application, in addition to the estimated tangential velocity along the diametrical position of the plate and the considered deviation of ±10%. The image acquisition for the angular velocity of 180 RPM (Figure 7a) at 240 fps presented a tendency of the estimated curve up to approximately 0.08 m of the diametrical position equivalent to a tangential velocity of 0.7 m/s; meanwhile, the acquisition with 960 fps has revealed a linear trend of the estimated value up to 0.095 m of the plate diameter, equivalent to a tangential velocity of about 0.85 m/s.

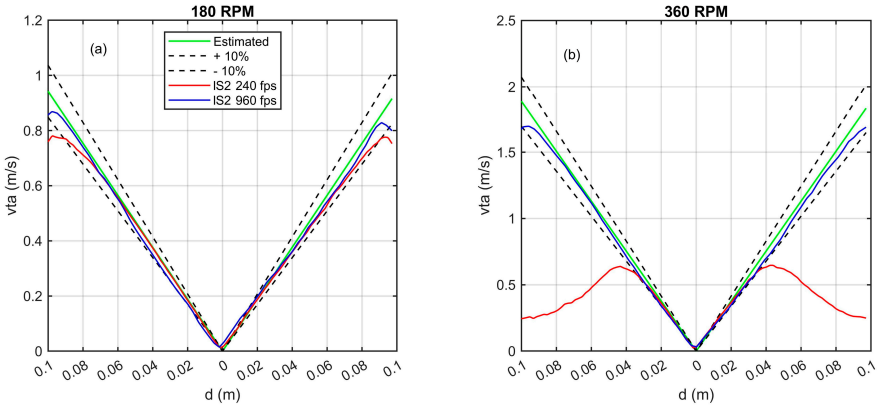

Figure 7. Analysis of velocimetry data for the configurations formed by IS2 at 240 fps and 960 fps and plate angular velocities at (**a**) 180 RPM and (**b**) 360 RPM.

It is also possible to visualize a deviation of the result in relation to the trend of the estimated value in Figure 7a, relating the upper and lower parts of the plate. The top part of the plate should give identical or similar results to the bottom part of the plate, as the circular motion is uniform, and the image sensor is centered on the plate. Despite being a systematic error, the reason for this is still unknown, and may be related to some noise in the images arising from non-uniformity in the lighting on the plate, suggesting that it should be better evaluated in future studies.

The absolute tangential velocity observed in the test with an acquisition rate of 240 fps for an angular velocity of 360 RPM (Figure 7b) trends towards an estimated velocity up to approximately 0.04 m of the diametrical position, equivalent to the tangential velocity of 0.7 m/s. The acquisition with 960 fps presents a tangential velocity consistent with the estimate up to approximately 0.095 m diametrical position, equivalent to a tangential velocity of 1.7 m/s. These values confirm the qualitative result observed in Figure 6c,d, evidencing the significant differences in the vector field for the acquisition rates of 240 fps and 960 fps.

Furthermore, it is possible to visualize a small deviation in the diametrical end of the plate in both Figure 7a,b. This fact occurs due to the masking procedure of the remainder of the visual field. Therefore, the interrogation intervals at the edges of the plate are interpolated with null vectors from neighboring interrogation windows.

3.3. Comparative Analysis for Different Angular Velocities in SSM Mode Using IS2

The highest image recording rate available in the experimental apparatus of 960 fps was evaluated and the analysis was conducted with different angular speeds of the plate. The aim was to increase the angular velocity of the plate to a value in which the observed

results of the vector field begin to diverge from the estimated tangential velocity according to the known displacement.

Commercial systems provide specific equipment to apply the PIV technique, among which it is possible to highlight high-speed cameras. As an example, a study [32] reports the use of a camera performing image acquisition at 500,000 fps to analyze the core of a turbulent round jet. However, following a low-cost approach, we used the Samsung Galaxy S20 Fe smartphone in SSM mode with the ability to capture 960 fps, as this smartphone is currently among the devices with the highest capture speeds.

The angular velocities set for this analysis were 90, 180, 360, 720 and 960, with accuracies of ±(0.05% + 0.1 RPM) and 1200 RPM with an accuracy of ±(0.05% + 1 RPM). The acquisitions were performed in increasing order of angular speed while the other parameters were maintained, including keeping the smartphone's positioning unchanged between experiments.

Figure 8 presents the qualitative results of the plate vector field for the different adjusted angular velocities. Figure 8a–d correspond to rotational speeds of 90, 180, 360, and 720 RPM, respectively. Reinforcing this analysis, a 100% increment in angular velocity was applied in each experiment relative to the previous one. Consequently, it was observed that the magnitude of the maximum tangential velocity varied between 0.4 m/s, 0.8 m/s, 1.5 m/s, and 3 m/s, respectively, maintaining linear coherence across the four angular velocity levels analyzed

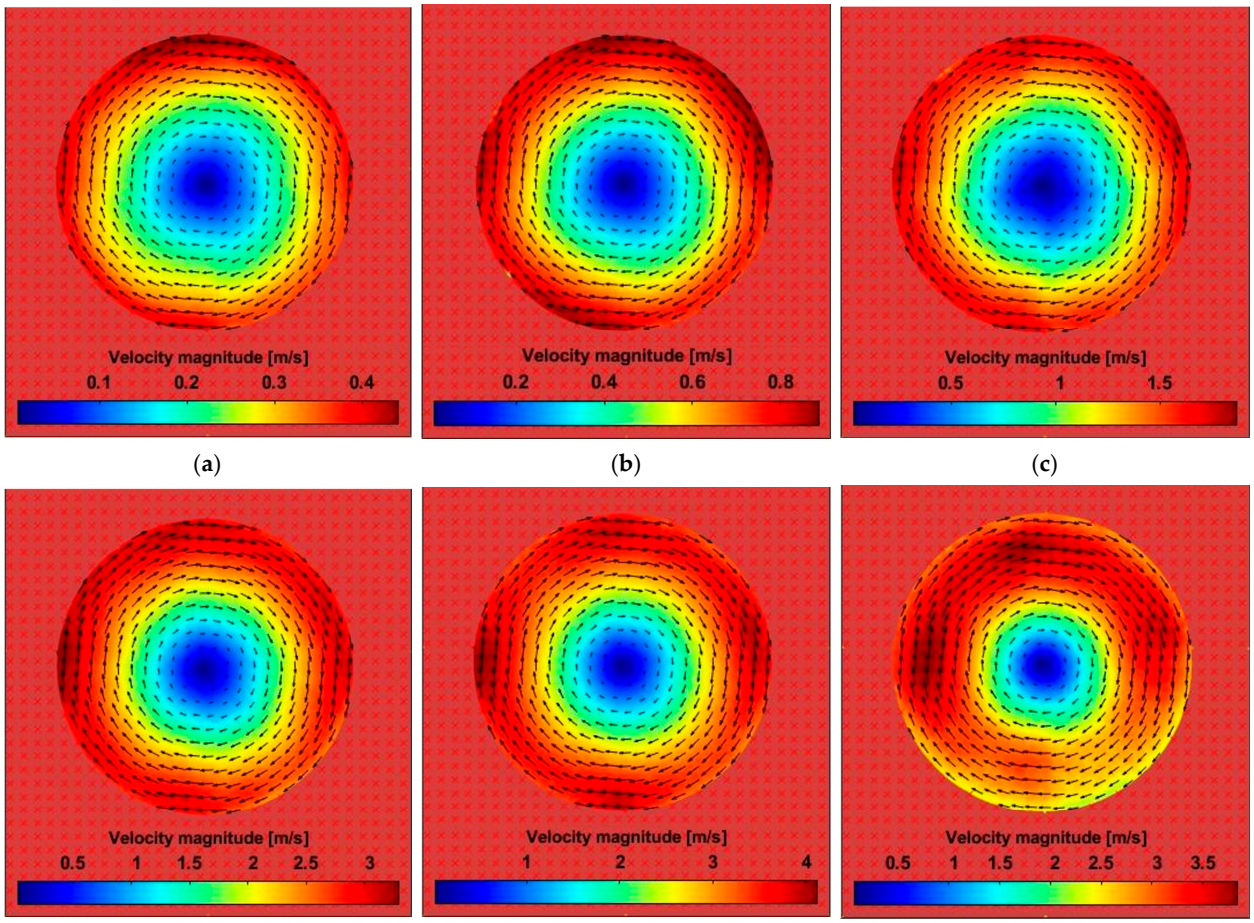

Figure 8. Velocity fields obtained with the PIVlab-MatLab® application from images captured with IS2 at 960 fps and different angular velocity settings: (**a**) 90 RPM; (**b**) 180 RPM; (**c**) 360 RPM; (**d**) 720 RPM; (**e**) 960 RPM and (**f**) 1200 RPM.

Furthermore, Figure 8e refers to the angular velocity of the plate at 960 RPM, in which the vector field increased between the center and the edge of the plate; considering a linear velocity curve, it is possible to state that the maximum absolute tangential velocity is consistent with the physics of reality, because the result is also proportional to the increments in the previous angular velocities.

Finally, Figure 8f was produced using a plate rotation speed of 1200 RPM, resulting in a heterogeneous velocity field for the same diametrical position. Thus, it is considered totally uncertain and unnecessary to carry out acquisitions with rotation speeds greater than 1200 RPM, as the measurement system was not capable of reproducing effective results.

Quantitative results can be obtained from the corresponding analysis of Figure 9. Figure 9a–d were produced using angular plate speeds at 90 RPM, 180 RPM, 360 RPM and 720 RPM, respectively, and we can see the tangential velocity increases as the angular velocity increases, reaching a maximum value near the edge of the plate.

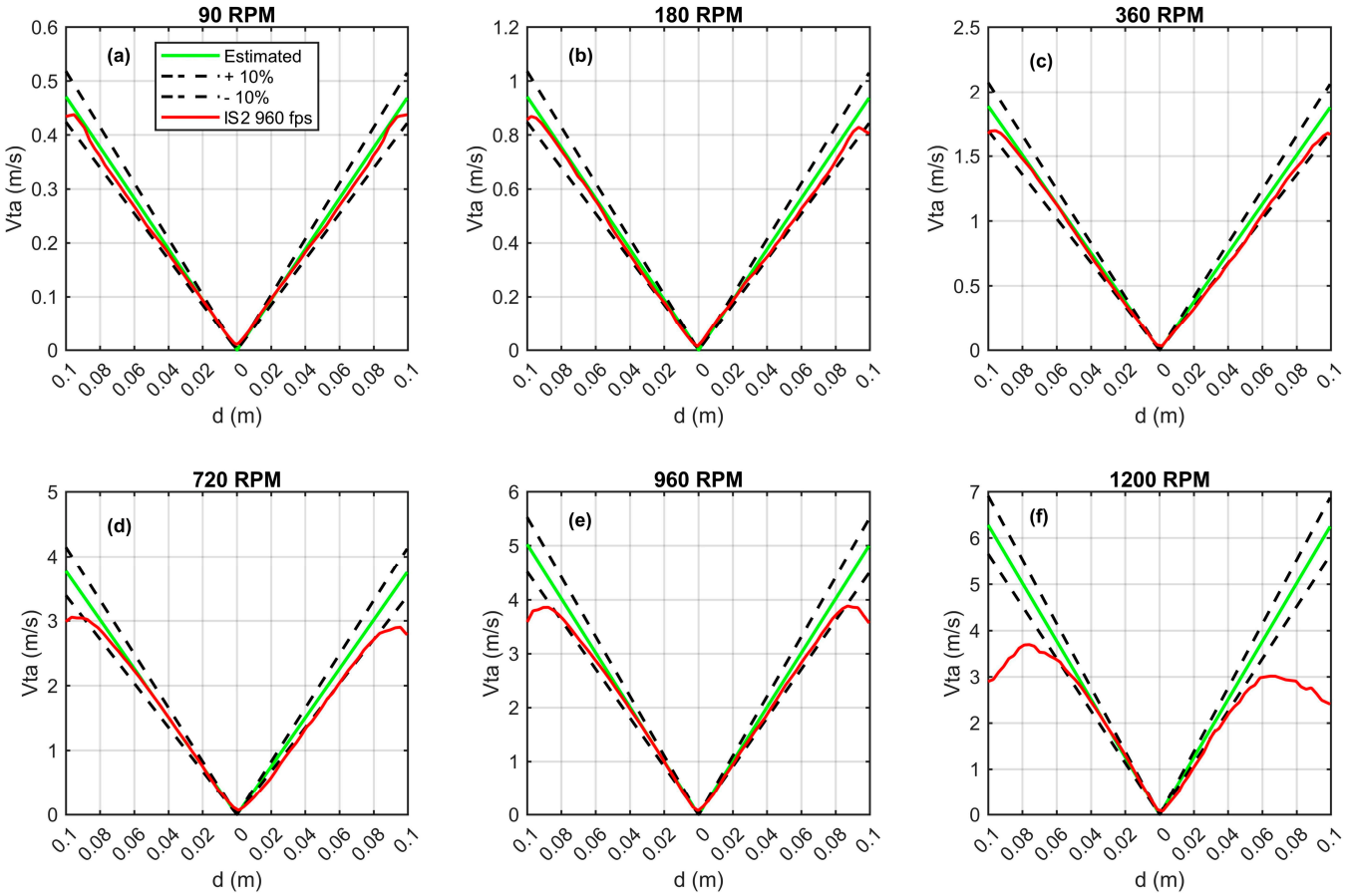

Figure 9. Analysis of velocimetry data for configurations formed by IS2 at 960 fps and plate angular velocity at: (**a**) 90 RPM; (**b**) 180 RPM; (**c**) 360 RPM; (**d**) 720 RPM; (**e**) 960 RPM and (**f**) 1200 RPM.

However, for 960 RPM, shown in Figure 9e, the maximum tangential velocity was approximately 3.8 m/s, corresponding to approximately 0.08 m in the plate diameter. The maximum tangential velocity obtained with an angular velocity of 1200 RPM in Figure 9f was 3.6 m/s in the upper part and 3 m/s in the lower part of the plate. In this case, and similarly to the qualitative analysis of Figure 8f, there was no uniformity throughout the diametrical range of the plate for the angular speed of 1200 RPM. Thus, the measurement system is unable to provide consistent results for the entire area of the plate due to the increase in the displacement speed of the particles. In turn, it is possible to visualize that

the deviation of the tangential velocity, considering a deviation of ±10%, starts around 3.8 m/s for 960 RPM and 3.0 m/s for 1200 RPM.

4. Conclusions

The image velocimetry analysis of synthetic particles with known displacement is useful in evaluating the applicability of the PIV technique using alternative methods for image acquisition, such as the use of smartphones. In addition, several software programs and algorithms can be analyzed and validated using the known displacement of synthetic particles. In this study, three different analyses were performed.

The first analysis compared the use of two image acquisition systems, called IS1 and IS2, with an acquisition rate of 240 fps. In this case, both devices presented satisfactory results up to approximately 0.7 m/s of tangential velocity.

The second analysis only considered the use of IS2, comparing the acquisition mode in slow motion (240 fps) with the SSM acquisition mode (960 fps). While the acquisition with 240 fps showed deviations from the estimated velocity after a value around 0.7 m/s, the results in SSM mode (960 fps) are consistent up to the maximum admitted velocity of 1.8 m/s, or a plate angular speed of 360 RPM.

The third analysis compared different angular speeds of the plate using the highest image acquisition rate of IS2, which was 960 fps in SSM mode. According to the presented results, the tangential velocities of the synthetic particles used in the analyses with angular velocities of 90, 180, 360 and 720 RPM were similar to the estimated values. In addition, we observed deviations for tangential velocities greater than 3.5 m/s in the 960 RPM and 1200 RPM setups. Thus, according to the characteristics and experimental configurations, we assume that the proposed PIV measurement system was able to reproduce velocimetry results up to 3.5 m/s, or up to 3 m/s assuming a conservative analysis. However, an experimental procedure that guarantees enough samples for statistical conclusions must be considered.

Finally, this study demonstrated the feasibility of using smartphones as image acquisition devices for the PIV technique, especially in low-cost applications and educational contexts. The analyzed devices present reliable results for tangential velocities up to 3.5 m/s. Although limitations related to image quality and algorithms were observed at higher speeds, the proposed methodology offers an affordable solution for teaching and experiments with low-speed flows.

In future work, it would be interesting to expand the study to different diameters and concentrations of synthetic particles in the disk, evaluate the use of smartphones as image acquisition systems in a PIV application in a wind tunnel (respecting the limits of flow velocity, dimensions and particle concentration reported in this article), and propose an experimental procedure for applying the apparatus presented in fluid mechanics teaching activities.

Author Contributions: Conceptualization, A.G.G., S.K.J. and J.P.d.S.F.; methodology, S.K.J. and J.P.d.S.F.; data acquisition, A.G.G.; software, A.G.G.; validation, A.G.G., S.K.J. and J.P.d.S.F.; investigation, A.G.G.; data curation, A.G.G.; writing—original draft preparation, A.G.G.; writing—review and editing, J.P.d.S.F., S.K.J. and F.P.M.; visualization, J.P.d.S.F.; supervision, J.P.d.S.F.; project administration, F.P.M.; funding acquisition, F.P.M. All authors have read and agreed to the published version of the manuscript.

Funding: This research was funded by FURNAS Centrais Elétricas and Research and Technological Development Program (P&D) of ANEEL, grant number ANEEL PD-00394-1906/2019.

Institutional Review Board Statement: Not applicable.

Data Availability Statement: The data presented in this study are available on request from the corresponding author. The data are not publicly available due to contractual restrictions established with the funder.

Acknowledgments: The authors would like to thank FURNAS Centrais Elétricas and the "Programa de Pesquisa e Desenvolvimento Tecnológico" (P&D) of the ANEEL for the financial support. The authors are grateful to EMC-UFG for the available infrastructure as well as for the administrative and technical support.

Conflicts of Interest: The authors declare that this study received funding from FURNAS Centrais Elétricas. The funder was not involved in the study design, collection, analysis, interpretation of data, the writing of this article or the decision to submit it for publication.

References

1. Mayinger, F.; Feldmann, O. *Optical Measurements, Techniques and Applications*, 2nd ed.; Springer: New York, NY, USA, 2001. [CrossRef]
2. Dracos, T. *Three-Dimensional Velocity and Vorticity Measuring and Image Analysis Techniques*, 1st ed.; Springer: Zurich, Switzerland, 1996. [CrossRef]
3. Sijie, F.; Pascal, H.B.; Christian, M. Particle tracking velocimetry for indoor airflow field: A review. *Build. Environ.* **2015**, *87*, 34–44. [CrossRef]
4. Girardi, G.A.; Kitatani Júnior, S.; Fonseca, J.P.S. A review of particle image velocimetry techniques. In Proceedings of the 26th International Congress of Mechanical Engineering, Florianópolis, Brazil, 22–26 November 2021. [CrossRef]
5. Cierpka, C.; Hain, R.; Buchmann, N.A. Flow visualization by mobile phones cameras. *Exp. Fluids* **2016**, *57*, 108. [CrossRef]
6. Käufer, T.; König, J.; Cierpka, C. Stereoscopic PIV measurements using low-cost action cameras. *Exp. Fluids* **2021**, *62*, 57. [CrossRef]
7. Aguirre-Pablo, A.A.; Alarj, M.K.; Li, E.Q.; Hernández-Sánchez, J.F.; Thoroddsen, S.T. Tomographic particle image velocimetry using smartphones and colored shadows. *Sci. Rep.* **2017**, *7*, 3714. [CrossRef]
8. Cierpka, C.; Otto, H.; Poll, C.; Huther, J.; Jeschke, S.; Mader, P. SmartPIV: Flow velocity estimates by smartphones for education and field studies. *Exp. Fluids* **2021**, *62*, 172. [CrossRef]
9. Raffel, M.; Willert, C.E.; Scarano, F.; Kähler, C.J.; Wereley, S.T.; Kompenhans, J. *Particle Image Velocimetry: A Practical Guide*, 3rd ed.; Springer: Cham, Switzerland, 2018; pp. 218–219. [CrossRef]
10. Goldstein, R. *Fluid Mechanics Measurements*, 2nd ed.; Routledge: New York, NY, USA, 1996. [CrossRef]
11. Han, L.; Wang, H.; Liu, X.; Xie, R.; Mu, H.; Fu, C. Particle Image Velocimetry of Oil–Water Two-Phase Flow with High Water Cut and Low Flow Velocity in a Horizontal Small-Diameter Pipe. *Sensors* **2019**, *19*, 2702. [CrossRef]
12. Kim, G.B.; Je, J.H.; Lee, S.J. Synchrotron X-ray PIV Technique for Measurement of Blood Flow. Velocity. *AIP Conf. Proc.* **2007**, *879*, 1891–1894. [CrossRef]
13. Yang, Z.; Sarkar, P.; Hu, H. An Experimental Investigation on the Wake Characteristics of a Wind Turbine in an Atmospheric Boundary Layer Wind. In Proceedings of the 29th AIAA Applied Aerodynamics Conference, Honolulu, HI, USA, 27–30 June 2011. [CrossRef]
14. Carter, D.W.; Ganapathisubramani, B. Data-driven determination of low-frequency dipole noise mechanisms installed airfoils. *Exp. Fluids* **2023**, *64*, 41. [CrossRef]
15. Kleinhans, M.G.; Van Der Vegt, M.; Leuven, J.; Braat, L.; Markies, H.; Simmelink, A.; Roosendaal, C.; Van Eijk, A.; Vrijbergen, P.; Van Maarseveen, M. Turning the tide: Comparison of tidal flow by periodic sea level fluctuation and by periodic bed tilting in scaled landscape experiments of estuaries. *Earth Surf. Dyn.* **2017**, *5*, 731–756. [CrossRef]
16. Wu, Q.; Zhu, C.A.; Liu, L.; Liu, J.; Luo, Z. Two-dimensional flow visualization and velocity measurement in natural convection near indoor heated surfaces using a thermal image velocimetry method. *Appl. Therm. Eng.* **2019**, *146*, 556–568. [CrossRef]
17. Rousseau, G.; Ancey, C. Scanning PIV of turbulent flows over and through rough porous beds using refractive index matching. *Exp. Fluids* **2020**, *61*, 172. [CrossRef]
18. ITTC—International Towing Tank Conference. Recommended Procedures and Guidelines. Guideline on Best Practices for the Applications of PIV/SPIV in Towing Tanks and Cavitation Tunnels. 2014. Available online: https://www.ittc.info/media/9587/75-02-01-04.pdf (accessed on 28 July 2023).
19. Foucaut, J.M.; Miliat, B.; Perenne, N.; Stanislas, M. Characterization of different PIV algorithms using the EUROPIV synthetic image generator and real images from a turbulent boundary layer. In *Particle Image Velocimetry: Recent Improvements*, 1st ed.; Stanislas, M., Westerweel, J., Kompenhans, J., Eds.; Springer: Berlin/Heidelberg, Germany; New York, NY, USA, 2004; Volume 2, pp. 163–185. [CrossRef]
20. Willert, C.E.; Gharib, M. Digital particle image velocimetry. *Exp. Fluids* **1991**, *10*, 181–193. [CrossRef]

21. Wei, X.; Huang, B.; Kanemoto, T.; Wang, L. Near wake study of counter-rotating horizontal axis tidal turbines based on PIV measurements in a wind tunnel. *J. Mar. Sci. Technol.* **2017**, *22*, 11–24. [CrossRef]
22. Ullah, A.H.; Rostad, B.L.; Estevadeordal, J. Three-cylinder rotating system flows and their effects on a downstream dimpled airfoil. *Exp. Therm. Fluid. Sci.* **2021**, *124*, 110343. [CrossRef]
23. Al-Garni, A.M.; Bernal, L.P. Experimental study of a pickup truck near wake. *J. Wind. Eng. Ind. Aerodyn.* **2010**, *98*, 100–112. [CrossRef]
24. Olasek, K.; Karczewski, M. Velocity data-based determination of airfoil characteristics with circulation and fluid momentum change methods, including a control surface size independence test. *Exp. Fluids* **2021**, *62*, 108. [CrossRef]
25. Bardera, R.; Rodríguez-Sevillano, Á.; García-Magariño, A. Aerodynamic investigation of a morphing wing for micro air vehicle by means of PIV. *Fluids* **2020**, *5*, 191. [CrossRef]
26. Giovannetti, L.M.; Banks, J.; Turnock, S.R.; Boyd, S.W. Uncertainty assessment of coupled digital image correlation and particle image velocimetry for fluid-structure interaction wind tunnel experiments. *J. Fluids Struct.* **2017**, *68*, 125–140. [CrossRef]
27. Faria, A.F.; Avelar, A.C.; Fisch, G. Wind tunnel investigation of the wind patterns in the launching pad area of the Brazilian Alcântara Launch Center. *J. Aerosp. Technol. Manag.* **2019**, *11*, e0719. [CrossRef]
28. Tominaga, Y.; Okaze, T.; Mochida, A.; Sasaki, Y.; Nemoto, M.; Sato, T. PIV measurements of saltating snow particle velocity in a boundary layer developed in a wind tunnel. *J. Vis.* **2013**, *16*, 95–98. [CrossRef]
29. Thielicke, W.; Stamhuis, E.J. PIVlab—Towards user-friendly, affordable and accurate digital particle image velocimetry in MATLAB. *J. Open Res. Softw.* **2014**, *2*, e30. [CrossRef]
30. Ligus, G.; Wasilewski, M.; Kołodziej, S.; Zając, D. CFD and PIV investigation of a liquid flow maldistribution across a tube bundle in the shell-and-tube heat exchanger with segmental baffles. *Energies* **2020**, *13*, 5150. [CrossRef]
31. Smith, L.D., III; Conner, M.E.; Liu, B.; Dzodzo, B.; Paramonov, D.V.; Beasley, D.E.; Langford, H.M.; Holloway, M.V. Benchmarking computational fluid dynamics for application to PWR fuel. In Proceedings of the 10th International Conference on Nuclear Engineering, Arlington, VA, USA, 14–18 April 2002; pp. 823–830. [CrossRef]
32. Geschwindner, C.; Westrup, K.; Dreizler, A.; Bohm, B. Ultra-high-speed time-resolved PIV of turbulent flows using a continuously pulsing fiber laser. *Exp. Fluids* **2022**, *63*, 75. [CrossRef]

Disclaimer/Publisher's Note: The statements, opinions and data contained in all publications are solely those of the individual author(s) and contributor(s) and not of MDPI and/or the editor(s). MDPI and/or the editor(s) disclaim responsibility for any injury to people or property resulting from any ideas, methods, instructions or products referred to in the content.